

# On the Nature of the Active Site in bis(imino)Pyridyl Iron, a Catalyst for Olefin Polymerization

Jorge Martínez,<sup>†</sup> Víctor Cruz,<sup>‡</sup> Javier Ramos,<sup>‡</sup> Soledad Gutiérrez-Oliva,<sup>†</sup>  
Javier Martínez-Salazar,<sup>‡</sup> and Alejandro Toro-Labbé\*,<sup>†</sup>

*QTC, Departamento de Química Física, Facultad de Química, Pontificia Universidad Católica de Chile, Santiago, Chile, and GEMPPPO, Departamento de Física Macromolecular, Instituto de Estructura de la Materia, Consejo Superior de Investigaciones Científicas (CSIC), Serrano 113-bis. 28006–Madrid, España*

*Received: November 6, 2007; In Final Form: January 26, 2008*

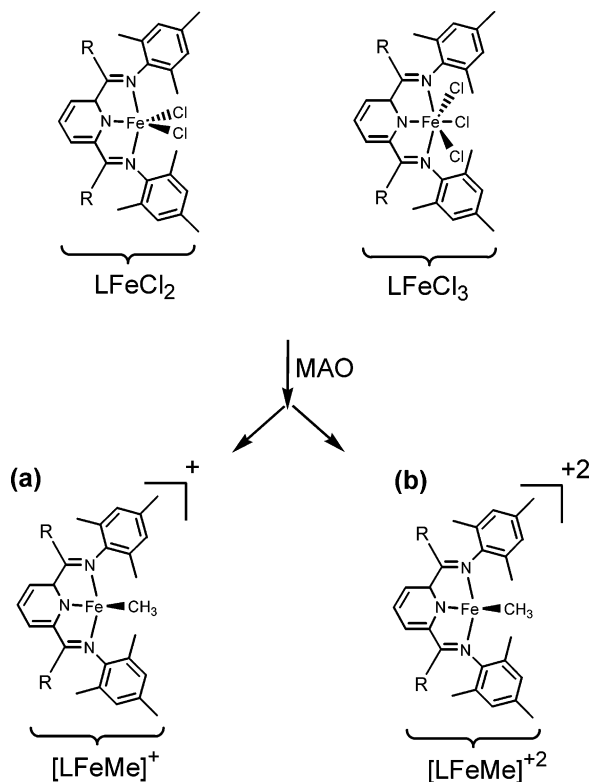
Global and local descriptors of chemical reactivity and selectivity are used in order to characterize the nature of the active species of bis(imino)pyridyl iron, a catalyst for olefin polymerization. It is shown that chemical potential, hardness, electrophilicity, as well as the dual and multiphilic descriptors for chemical reactivity and selectivity, are adequate for characterizing the global and local reactivity trends of this organo-metallic complex. Most theoretical evidence presented in this paper indicates that the catalyst of  $\text{Fe}^{+3}$  seems to be more active for olefin polymerization than that of  $\text{Fe}^{+2}$ . However, when the cocatalyst is considered, catalysts of  $\text{Fe}^{+2}$  and  $\text{Fe}^{+3}$  present similar electrophilic activity to orientate the nucleophilic attack. It is observed that this activity is well localized at the metallic center in the ferric species whereas it appears to be more delocalized on the ligands of the ferrous species.

## 1. Introduction

There is a great deal of interest in nonmetallocene catalytic systems since Brookhart et al.<sup>1</sup> and Gibson et al.<sup>2</sup> established the synthesis of highly active transition metal olefin polymerization catalysts based on iron. The catalysts are stabilized by bis(imino)pyridine ligands [ $\text{L}=2,6-(2,6-(\text{R})_2\text{C}_6\text{H}_4\text{N}=\text{CR}')_2\text{C}_5\text{H}_3\text{N}]^1$  affording highly linear polyethylene, whose density, molecular weight, and molecular weight distribution fall within the range of commercially relevant high-density polyethylenes (HDPEs).<sup>3</sup> However, the nature of active species for olefin polymerization is still a matter of debate. Motivated by two experimental studies that show controversy on the ferrous or ferric nature of the active center in bis(imino)pyridyl iron, in the present paper, global and local reactivity and selectivity descriptors, that come out from density functional theory (DFT),<sup>4,5</sup> are used to characterize the reactive nature of the active species. In particular, since the reactivity of the catalyst is basically played at a local level through the metallic center, it is important to characterize its electrophilic power by means of an adequate descriptor; this is the dual descriptor for reactivity and selectivity<sup>6</sup> that has been successfully used in the characterization of the reactivity in organic species.<sup>7</sup>

Theoretical studies indicate that monoalkyl  $\text{Fe}^{+2}$  and monoalkyl  $\text{Fe}^{+3}$  catalytic species<sup>8–10</sup> present similar activities producing polymers with the same overall characteristic properties. The two precursors,  $\text{LFeCl}_2$  and  $\text{LFeCl}_3$ , displayed in Scheme 1 were prepared and characterized through Mössbauer, electron paramagnetic resonance (EPR), and nuclear magnetic resonance (NMR) techniques.<sup>8,11</sup> The Mössbauer signals gave results consistent with  $d^6$  high-spin  $\text{Fe}^{+2}$  systems, that is,  $\text{LFeCl}_2$ ; for the  $\text{LFeCl}_3$ , the signal lies in the typical range for  $d^5$  high-spin  $\text{Fe}^{+3}$  systems. However, after activation of the precursors with

**SCHEME 1:** Precursors Used in the Experimental Works (a) by Gibson et al.<sup>8</sup> (with  $\text{R} = \text{H}$ ) and (b) by Talsi et al.<sup>11</sup> (with  $\text{R} = \text{CH}_3$ )



the methyl aluminoxane (MAO) cocatalyst, the Mössbauer spectra indicated the presence of the high-spin  $\text{Fe}^{+3}$  species only; no trace of the  $\text{Fe}^{+2}$  species was detected. Moreover, since  $\text{Fe}^{+2}$  is EPR silent, an analysis by using this technique has revealed that after activation of  $\text{LFeCl}_2$  by MAO an EPR spectrum was

\* Corresponding author.

<sup>†</sup> Pontificia Universidad Católica de Chile.

<sup>‡</sup> Instituto de Estructura de la Materia.

obtained, thus indicating that an oxidative process took place activated by MAO leading to  $\text{Fe}^{+3}$  as the active species.<sup>8</sup>

In spite of all information given above, Talsi et al.<sup>11</sup> claim that  $^1\text{H}$  NMR and EPR studies indicate that structures of  $\text{LFeCl}_2$  (bis(imino)pyridyl  $\text{Fe}^{+2}$ ) and  $\text{LFeCl}_3$  (bis(imino)pyridyl  $\text{Fe}^{+3}$ ) are converted under treatment with MAO into ferrous complexes  $[\text{LFe(II)}(\mu\text{-Me})_2\text{AlMe}_2]^+$  or  $[\text{LMeFe(II)}(\mu\text{-Me})_2\text{AlMe}_2]$ , depending on the Al/Fe ratio. In short, Talsi et al.<sup>11</sup> suggest that the  $\text{AlMe}_3$  group present in MAO cocatalyst would reduce rather than oxidize iron precursors, in contrast with the EPR results.<sup>8</sup> In spite of this controversy, there are studies on the kinetic of the polymerization reaction<sup>12</sup> supporting the idea that active centers presenting different oxidation states could participate in the polymerization process, this might be explaining the broad molecular weight distribution usually obtained with this kind of catalyst. Most relevant is the work of Gambarotta et al.<sup>13,14</sup> showing that the reactivity of these catalysts may be centered not only in the metal but also in the bis(imino)pyridine ligand.

In the light of the above open discussion, in this paper, global and local reactivity descriptors<sup>4,5</sup> are used to analyze the different active species proposed so far with the aim of identifying the catalyst that is more suitable for the olefin polymerization. Polymerization reactions are very complex dynamical processes; many factors may play crucial roles in the characterization of the whole process. In this paper, we will consider the intrinsic reactivity of the isolated catalytic species knowing that it can be modified because of specific interactions that arise during the course of the reaction.<sup>15</sup> These interactions may be of different types, and specific reactivity descriptors adapted to them have been recommended.<sup>16</sup>

## 2. Theoretical Background

Conceptual DFT<sup>4,5</sup> has provided a set of reactivity indexes based on the fact that the electronic energy  $E$  can be written as a functional of  $N$  (the total number of electrons) and  $v(\mathbf{r})$  (the external potential):  $E \equiv E[N, v(\mathbf{r})]$ . Assuming differentiability of  $E$  respect to  $N$  and  $v(\mathbf{r})$ , a series of response functions emerge: the chemical potential,  $\mu$ , characterizing the escaping tendency of electrons from equilibrium is defined as:<sup>4,5,17</sup>

$$\mu = \left( \frac{\partial E}{\partial N} \right)_{v(\mathbf{r})} = -\chi \quad (1)$$

the link between DFT and classical chemistry is achieved when chemical potential is defined as the negative of the electronegativity ( $\chi$ ) of the system,<sup>18</sup> as indicated in eq 1. Molecular hardness,  $\eta$ , is the resistance to charge transfer, and it is defined as<sup>4,5,17</sup>

$$\eta = \left( \frac{\partial^2 E}{\partial N^2} \right)_{v(\mathbf{r})} \quad (2)$$

Both,  $\mu$  and  $\eta$  are global properties that are implicated in the reactivity of molecular systems.<sup>15,19–23</sup> A three-point finite difference approximation leads to the following working definitions of these properties:<sup>4,5</sup>

$$\mu \approx -\frac{1}{2}(I + A); \quad \eta \approx \frac{1}{2}(I - A) \quad (3)$$

where  $I$  and  $A$  are the first vertical ionization potential and electron affinity of the neutral molecule, respectively. Further approximation using the Koopman's theorem<sup>24</sup> ( $I \approx -\epsilon_{\text{H}}$  and  $A \approx -\epsilon_{\text{L}}$ ) allows one to write  $\mu$  and  $\eta$  in terms of the energy of

the lower unoccupied and higher occupied molecular orbitals, LUMO ( $-\epsilon_{\text{L}}$ ) and HOMO ( $\epsilon_{\text{H}}$ ), respectively:

$$\mu \approx \frac{1}{2}(\epsilon_{\text{L}} + \epsilon_{\text{H}}); \quad \eta \approx \frac{1}{2}(\epsilon_{\text{L}} - \epsilon_{\text{H}}) \quad (4)$$

Following Parr et al.,<sup>25</sup> the square of the chemical potential of a chemical species divided by two times its chemical hardness, defines its electrophilicity index:<sup>25</sup>

$$\omega = \mu^2/2\eta \quad (5)$$

that measures the energetic stabilization when the system gets electrons from the surroundings.

On the other hand, the variation of the energy with respect to the external potential, without charge transfer, leads to the electronic density  $\rho(\mathbf{r})$  at first order and to the Fukui function  $f(\mathbf{r})$  at second order;<sup>5,26</sup> both the electronic density and Fukui function are local quantities. The Fukui function,  $f(\mathbf{r})$ , describes the local changes in the electron density of the system due to the perturbation in the global number of electrons; this is obtained through a Maxwell relationship:<sup>5,26</sup>

$$f(\mathbf{r}) = \left[ \frac{\delta \mu}{\delta v(\mathbf{r})} \right]_N = \left( \frac{\partial \rho(\mathbf{r})}{\partial N} \right)_{v(\mathbf{r})} \quad (6)$$

$f(\mathbf{r})$  reflects the ability of a molecule to accept (donate) electrons from (to) another system. It can be observed in eq 6 that high values of  $f(\mathbf{r})$  are due to large variations of  $\mu$  which entails high reactivity at point  $\mathbf{r}$  because of the electron transfer induced by the variation of chemical potential.<sup>27</sup> Since the number of electrons  $N$  is a discrete variable, left and right derivatives of the density with respect to  $N$  are performed and then approximated using the finite difference approximation. Two Fukui functions emerge:  $f^+(\mathbf{r})$  defining the reactivity at point  $\mathbf{r}$  toward a nucleophilic attack that increases the number of electrons of the system and  $f^-(\mathbf{r})$  defining the reactivity at point  $\mathbf{r}$  toward an electrophilic attack that decreases the number of electrons of the system.<sup>27</sup> When the frozen orbital approximation (FOA) is imposed,<sup>28</sup>  $f^+(\mathbf{r})$  and  $f^-(\mathbf{r})$  are written in terms of the density of the lowest unoccupied and highest occupied molecular orbitals: LUMO for the incoming electrons and HOMO for the outgoing electrons<sup>27,29</sup>

$$f^+(\mathbf{r}) \approx \rho^{\text{LUMO}}(\mathbf{r}); \quad f^-(\mathbf{r}) \approx \rho^{\text{HOMO}}(\mathbf{r}) \quad (7)$$

Condensed to atoms, Fukui descriptors (or indexes) can be obtained through integration within the atomic domain  $\Omega_k$  for atom  $k$ :<sup>30</sup>

$$f_k^{+/-} = \int_{\Omega_k} f^{+/-}(\mathbf{r}) d\mathbf{r} \quad (8)$$

Recently, a new dual descriptor for chemical reactivity has been proposed.<sup>6,7,31</sup> It is defined in terms of the variation of hardness with respect to the external potential and it is approached by the difference between nucleophilic and electrophilic Fukui functions:

$$\Delta f(\mathbf{r}) = \left[ \frac{\delta \eta}{\delta v(\mathbf{r})} \right]_N \approx [f^+(\mathbf{r}) - f^-(\mathbf{r})] \approx [\rho^{\text{LUMO}}(\mathbf{r}) - \rho^{\text{HOMO}}(\mathbf{r})] \quad (9)$$

thus allowing to obtain simultaneously the nucleophilic and the electrophilic trend of reactivity at point  $\mathbf{r}$ . A spin version ( $\alpha$  or  $\beta$ ) of the dual descriptor should be used for open shell systems, as in the present case. This can be achieved by putting in eq 9

the appropriate densities associated to the highest occupied and lower unoccupied orbitals,  $\alpha$  or  $\beta$ . After integrating over the domain  $\Omega_k$  the condensed dual descriptor is obtained:

$$\Delta f_k = \int_{\Omega_k} \Delta f(\mathbf{r}) \, d\mathbf{r} = (f_k^+ - f_k^-) \quad (10)$$

so that when  $\Delta f_k > 0$ , the process is driven by a nucleophilic attack on atom  $k$  and this atom acts as an electrophilic species; conversely, when  $\Delta f_k < 0$ , the process is driven by an electrophilic attack over atom  $k$  and it acts as a nucleophilic species. Since the dual descriptor gives only local information, the multiphilic descriptor which is a combination of the global electrophilicity index and the dual descriptor:<sup>32</sup>

$$\Delta\omega_k = \omega \cdot \Delta f_k \quad (11)$$

will also be used to characterize the reactivity of the catalyst. Because of its global information content through the electrophilicity index,  $\Delta\omega_k$  is expected to complement the local information contained in  $\Delta f_k$ . Both,  $\Delta f_k$  and  $\Delta\omega_k$  have been used successfully in the characterization of the reactivity of many systems.<sup>6,7,32</sup>

### 3. Computational Methods

For geometrical optimizations, Becke 88 for exchange and P86 for correlation functionals were used (BP86)<sup>33,34</sup> with the DZP basis set for the cationic complex  $[\text{LFeMe}]^{+2}$  which is a  $d^5$  high-spin  $\text{Fe}^{+3}$  site with  $S = 5/2$  and  $[\text{LFeMe}]^+$  which is a  $d^6$  high-spin  $\text{Fe}^{+2}$  with  $S = 2$ . DMol<sup>35,36</sup> within the Material-Studio<sup>37</sup> software package programs were used. After optimization was completed, the functionals used in single point calculations were the Becke-3 for exchange and Lee–Yang–Parr for correlation (B3LYP);<sup>38–41</sup> LANL2DZ pseudo-potential were used for the Fe atom, and the standard 6-31G(d) basis set was used for nonmetallic atoms. We tested in one case that the B3LYP/LANL2DZ/BP86/DZP model produced quite the same geometries and energies as the full optimization with the B3LYP/LANL2DZ model. Calculations were performed using Gaussian 03<sup>42</sup> and the Fukui functions were determined through a modified version of link 601.<sup>30</sup> In all cases, the most active orbitals associated to molecular reactivity (highest occupied and lower unoccupied) produced by the unrestricted scheme of calculation were of  $\beta$  spin, and therefore the dual descriptor was determined using the  $\beta$  densities of the frontier orbitals. Condensation of the dual descriptor for the bare catalyst was performed using the Mulliken condensation scheme.

### 4. Results and Discussions

The initial  $\text{LFeCl}_2$  precursor and the bare catalyst, as well as a model of the expected active species after MAO addition, are displayed in Figure 1; the latter two species are the subject of the present study. Note that slightly different structures to those studied here have been the subject of the experimental works by Gibson et al.<sup>8</sup> and by Talsi et al.;<sup>11</sup> however, they are close enough to allow a qualitative comparison among theoretical and experimental data. The resulting composite system catalyst MAO is expected to be cationic, it must provide enough room for an incoming monomer and an adequate electrostatic environment for olefin approach. However, as already mentioned, there is no certainty about the structure of the active species, specifically, the correct spin and oxidation state of the Fe atom. The following sections gather results that give important insights on the nature of the bis(imino)pyridyl iron catalyst for olefin polymerization.

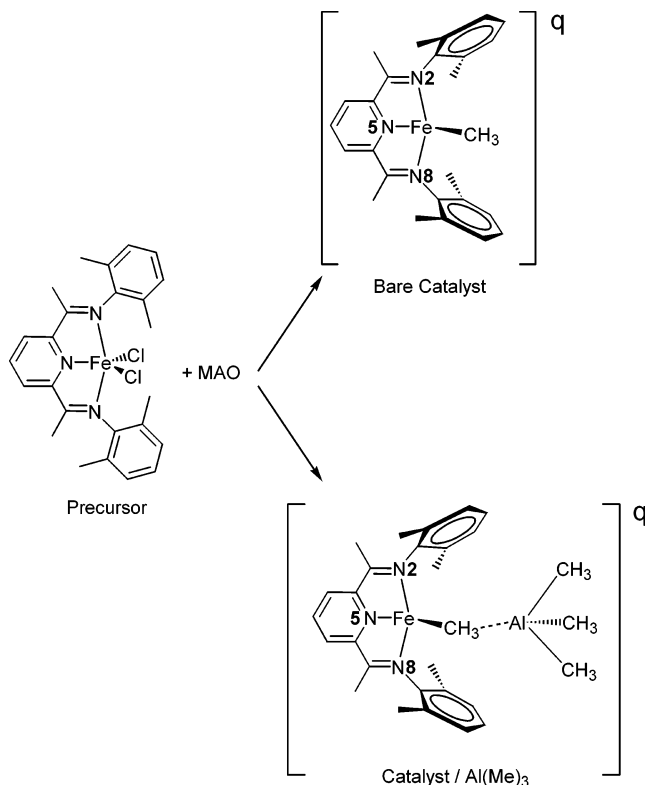


Figure 1. Molecular model for the catalyst used in this investigation.

TABLE 1: Spin–Chemical Potential, Hardness, and Electrophilicity Indexes for the bis(imino)Pyridyl Iron Catalyst Where the  $\Delta\mu$  Value Is Referred to the Chemical Potential of Ethylene,  $\mu = -78.45 \text{ kcal}\cdot\text{mol}^{-1}$ , and All Values Are Given in  $\text{kcal}\cdot\text{mol}^{-1}$

property	$\text{Fe}^{+2}$ ( $S = 2$ )	$\text{Fe}^{+3}$ ( $S = 5/2$ )	$\text{Fe}^{+2}-\text{Al}(\text{Me})_3$	$\text{Fe}^{+3}-\text{Al}(\text{Me})_3$
$\mu^\alpha$	-159.70	-248.70	-169.24	-160.31
$\mu^\beta$	-170.59	-262.97	-172.59	-171.77
$\bar{\mu}$	-165.15	-255.84	-170.92	-166.31
$\Delta\mu$	86.70	177.39	92.47	87.59
$\eta^\alpha$	27.69	31.03	31.65	25.98
$\eta^\beta$	29.38	16.30	28.73	27.70
$\bar{\eta}$	28.54	23.67	30.19	26.84
$\bar{\omega}$	477.0	1382.6	483.8	515.3

**4.1. Global Reactivity.** Because of the open shell configuration of the metallic complexes, the reactivity will be characterized through a set of spin descriptors  $\{\mu_\alpha, \eta_\alpha; \mu_\beta, \eta_\beta\}$ ; they are displayed in Table 1. Spin-average values of chemical potential ( $\bar{\mu}$ ) and hardness ( $\bar{\eta}$ ) were obtained and quoted in Table 1.

It can be observed in Table 1 that the effect of the cocatalyst on  $\text{Fe}^{+2}$  and  $\text{Fe}^{+3}$  species is opposite, whereas chemical potential is slightly lowered by the action of the cocatalyst in the ferrous species, it is dramatically increased in the ferric species. The overall effect of the cocatalyst seems to be the equalization of the global reactivity of both species.

Polymerization reaction is basically an electron-transfer reaction in which the olefin acts as an electron donor and the catalyst acts as electron acceptor; it is well-known that the larger the difference of  $\mu$  between two reacting species, the larger is the electron transfer among them.<sup>4,5,43,44</sup> In this context, the reactive capabilities of the catalysts is better appreciated relative to the partner species, ethylene. The chemical potential of ethylene is  $-78.45 \text{ kcal}\cdot\text{mol}^{-1}$  at the B3LYP/6-31G(d,p) level so that the largest difference in chemical potential is observed with the catalyst of  $\text{Fe}^{+3}$ . Therefore, bare  $\text{Fe}^{+3}$  species appear

**TABLE 2: Condensed Dual and Multiphili<sup>a</sup> Descriptors for the Reactive Sites of the Bare Catalyst of Fe<sup>+2</sup> and Fe<sup>+3</sup>**

<i>k</i>	$\Delta f_k$ (Fe <sup>+2</sup> )	$\Delta f_k$ (Fe <sup>+3</sup> )	$\Delta \omega_k$ (Fe <sup>+2</sup> )	$\Delta \omega_k$ (Fe <sup>+3</sup> )
Fe	−0.7018	0.6052	−334.76	836.75
N2	0.0649	0.0102	30.96	14.10
N5	0.1678	0.0268	80.04	37.05
N8	0.0653	0.0085	31.15	11.75

<sup>a</sup> In kcal·mol<sup>−1</sup>.

to be much more reactive than the corresponding Fe<sup>+2</sup> species. On the other hand, the presence of the cocatalyst practically equalize the charge-transfer power of ferrous and ferric species when reacting with ethylene.

Since molecular hardness is a measure of the resistance to charge transfer, the lower the hardness, the higher the reactivity; this is in line with the maximum hardness principle that asserts that molecular systems at equilibrium tend to states of high hardness.<sup>45–47</sup> In this context, it can be observed that the catalyst of Fe<sup>+3</sup> appears to be more reactive than Fe<sup>+2</sup> with and without the presence of cocatalyst. It is interesting to notice that, when including the cocatalyst in computational calculations through AlMe<sub>3</sub> coordinated to the catalyst, the values of spin-averaged hardness increase; the increment is larger in the Fe<sup>+3</sup>–cocatalyst system although this species is still more reactive than Fe<sup>+2</sup>–cocatalyst composite system. The cocatalyst somehow tends to equalize the resistance to charge transfer for both iron complex species, although this intrinsic global reactivity index favors the Fe<sup>+3</sup> (*S* = 5/2) species.

Values of averaged electrophilicity index are also quoted in Table 1. It can be observed that the catalyst of Fe<sup>+3</sup> is by far a better electrophile than the Fe<sup>+2</sup> species. When the cocatalyst is added, the electrophilicity of the Fe<sup>+2</sup> species remains quite unchanged whereas it drops dramatically in the case of the Fe<sup>+3</sup> catalyst, although it still remains as the better electrophile.

In summary, the difference of chemical potential among the reacting species indicates that in the absence of the cocatalyst, the Fe<sup>+3</sup> species appears to be most reactive for olefin polymerization. However, this clear-cut tendency is somewhat reversed in the presence of the cocatalyst. The criteria based on the principle of maximum hardness<sup>45–47</sup> and electrophilicity index<sup>25</sup> also suggests that the ferric species should be more active than the ferrous species.

**4.2. Local Reactivity.** **4.2.1. Bare Catalytic Species.** The dual descriptor of chemical reactivity and selectivity<sup>6</sup> is a useful tool to simultaneously quantify the nucleophilic and electrophilic behavior of a molecular site; Table 2 quotes the values of the dual index condensed to the main atoms that define the reactive region of the catalytic system. According to Figure 1, these atoms are Fe, N2, N5, and N8. We observe that for the Fe<sup>+2</sup> complex  $\Delta f_{\text{Fe}} = -0.7018$  indicating a surprisingly high tendency to act as a nucleophile, in complete contrast with the expected reactivity behavior of the metallic center which is that of an electrophile. This result predicting an electrophilic attack on Fe is not compatible with olefin coordination. On the other hand, it can be observed in Table 2 that the right nucleophilic attack is predicted on the metallic center in the Fe<sup>+3</sup> species; it presents the largest positive value of  $\Delta f_{\text{Fe}}$ . Since condensation of the dual descriptor may produce errors due to the condensation scheme in which one has to define arbitrarily the integration domain,<sup>30</sup> the dual descriptor is much better appreciated when displayed as three-dimensional maps, as the ones depicted in Figure 2 for the ferrous and ferric catalyst.

In Figure 2a, small positive lobes localized on the Fe<sup>+2</sup> cation appear surrounded by negative lobes of the dual descriptor thus

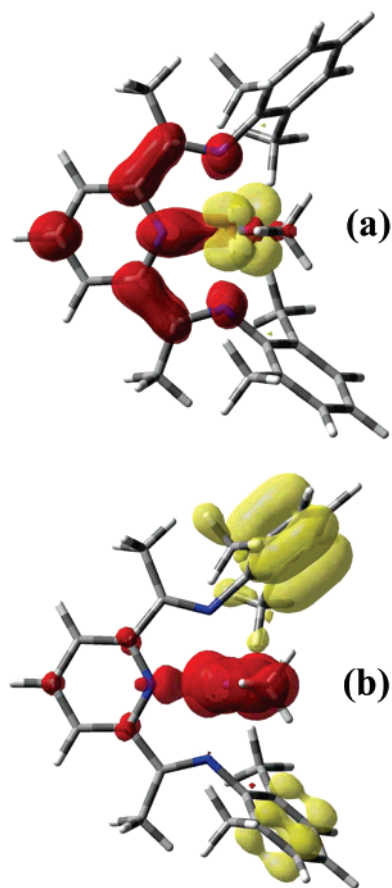


**Figure 2.** Isosurface at 0.002 au of the dual descriptor for the bare catalyst of (a) Fe<sup>+2</sup> and (b) Fe<sup>+3</sup>. In yellow are the nucleophilic regions, and in red are the electrophilic regions.

confirming the difficulty to define the atomic basins for a proper integration of eq 9 to obtain reliable values for the condensed dual descriptor. The electrophilic power of the metallic center is attenuated by the nucleophilic strength of the alkyl group beside it. Moreover, positive lobes are located around the imino ligands, on the N atom, and on the para-position of the pyridine substructure thus defining unexpected electrophilic sites. It appears that ligands are playing a main reactive role in the reaction with a nucleophile such as ethylene thus lowering the electrophilic power of the metallic center. This effect has been already observed by other authors and referred to as the non-innocent reactivity of the ligands;<sup>13,14</sup> this refers to ligands that are amenable to suffer nucleophilic and/or electrophilic attack, in addition to the expected reactivity of the metal center. As a result, the ligands may compete with the metallic center as a reaction site thus diminishing the efficiency of the catalyst. One important result that comes out from this analysis is that the dual descriptor identify nicely the innocent or non-innocent nature of ligands in front of the reaction partner.

Figure 2b shows the map of the dual descriptor for the catalyst of Fe<sup>+3</sup>. The positive lobes are well localized surrounding the metallic center thus indicating its aptitude to accept a nucleophilic attack. Here, the ligands do not show a noticeable activity. The non-innocent effect of the ligands is largely absent in the Fe<sup>+3</sup> complex so that a more efficient coordination of the olefin to the metallic center is then expected. In summary, although in both complexes, the Fe atom presents electrophilic capability that should orientate a nucleophilic attack, it is expected that the most reactive species is the Fe<sup>+3</sup> complex because its electrophilic activity is mostly concentrated on the metallic atom.



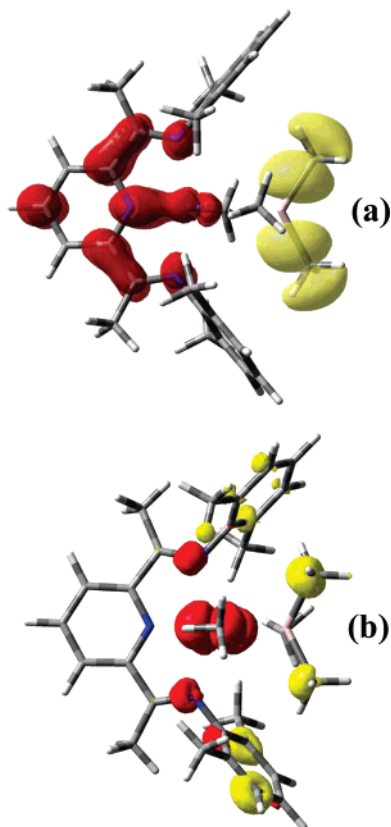


**Figure 3.** Isosurface at 0.002 au of the dual descriptor for the composite systems of (a)  $\text{Fe}^{+2}$  and (b)  $\text{Fe}^{+3}$ .

Ligands do not play the reactive role that diminish the electrophilic power of the  $\text{Fe}^{+2}$  catalyst.

Numerical values of the multiphilic descriptor condensed to the reactive atoms calculated using the averaged electrophilic index are also quoted in Table 2. One advantage of the multiphilic descriptor is that it provides higher values in terms of magnitude compared with the dual descriptor. In all cases, the overall trend displayed by the dual descriptor is conserved although the observed relative differences between the two catalyst in most cases are much more reduced. Following the multiphilic descriptor, the  $\text{Fe}^{+3}$  species appears to be the most active catalyst for olefin polymerization.

To confirm that the catalyst of  $\text{Fe}^{+2}$  or  $\text{Fe}^{+3}$  should be the active species for olefin polymerization, other species proposed in the literature<sup>48</sup> such as the anionic monomethylated complex  $[\text{LFeMe}(\text{eq})]^{-1}$  of  $\text{Fe}(0)$  were analyzed. We calculated the dual and multiphilic descriptors for different spin states of this compound with the result that only the  $S = 2$  high-spin  $\text{Fe}(0)$  state exhibited a rather small electrophilic lobe around the Fe atom. This result is therefore in line with the fact that the relevant species for olefin polymerization are those of  $\text{Fe}^{+2}$  and  $\text{Fe}^{+3}$ .

**4.2.2. Effect of the Cocatalyst.** Further calculations of the dual descriptor were performed on complexes which included an alkyl-aluminum moiety to model the cocatalyst as suggested by Talsi and co-workers.<sup>11</sup> The dual descriptor map of the optimized geometry of the  $\text{Fe}^{+2}$ -cocatalyst complex is shown in Figure 3a. Figure 3b gathers that of the  $\text{Fe}^{+3}$  species. It can be observed that, as for the bare system shown in Figure 2, the electrophilic character presents about the same features: in the ferrous catalyst, it remains delocalized mainly on the pyridine ring and in a lesser extent on the metallic center; in the ferric catalyst, the electrophilic character is much more localized on the metallic center.

In contrast to what is observed in Figure 2a, the nucleophilic behavior of the  $\text{Fe}^{+2}$  is now displaced toward the alkyl aluminum, far away from the metallic center thus contributing to enhance the efficiency of the Fe atom for a nucleophilic attack. The effect of the alkyl aluminum on the  $\text{Fe}^{+3}$  species is mostly associated with delocalization of the nucleophilic power of the catalyst. The dual descriptor shows that  $\text{Fe}^{+3}$  keeps its electrophilic nature as in the bare complex. The nucleophilic reactivity is however shared between the aryl substituents of the catalyst and the cocatalyst moiety. In summary, the dual descriptor reveals that the inclusion of the cocatalyst is essential to describe correctly the nucleophilic attack on the Fe atom; it practically equalizes the reactivity of the ferrous and ferric species thus making them good partners for olefin polymerization. This is in agreement with the experimental information given by Talsi and co-workers.<sup>11</sup>

## 5. Concluding Remarks

In this paper, two models of catalyst consisting of bare species of  $\text{Fe}^{+2}$  and  $\text{Fe}^{+3}$  and the corresponding complexes formed with the cocatalyst have been analyzed. The chemical potential, hardness, and electrophilicity criteria indicates that the  $\text{Fe}^{+3}$  species is more favorable because this complex is the most reactive and will induce the largest electron transfer with the olefin. The dual descriptor of local reactivity of the bare species shows unambiguously that  $\text{Fe}^{+3}$  is the preferred species for olefin polymerization because the electrophilic activity is largely localized at the metallic center, in contrast with the strong activity displayed by the ligands in the  $\text{Fe}^{+2}$  species. This result was confirmed by the multiphilic descriptor that contains simultaneously global and local reactivity information.

When the model of MAO cocatalyst comes to the picture, the catalytic activity of the  $\text{Fe}^{+3}$  species is modified dramatically making the  $\text{Fe}^{+3}$ -cocatalyst composite system as good as the  $\text{Fe}^{+2}$ -cocatalyst system; however, the latter presents a strong delocalization of the electrophilic power making the whole catalytic species of  $\text{Fe}^{+2}$  much less efficient than the  $\text{Fe}^{+3}$  catalytic species. These results showing the suitability of both  $\text{Fe}^{+2}$  and  $\text{Fe}^{+3}$  complexes for olefin polymerization are compatible with the general observation that active centers of different nature mediate in the polymerization process catalyzed with these compounds. The multi-center nature of the active species is supported by recent experimental results for the ethylene polymerization based on iron catalysts.<sup>12,48</sup>

**Acknowledgment.** The authors wish to thank Professor Juan Manuel Manríquez (PUC) for helpful discussions. This work has been supported by the following: FONDECYT Grant 1060590; FONDAP Grant 11980002 (CIMAT); Ministerio de Educación y Ciencia (Spain) Grant MAT2006-0400; Comunidad de Madrid Grant S-0505/PPQ-0328, and Collaboration Program CSIC-CONICYT. The authors also wish to thank CTI-CSIC (Madrid) and CESGA (Santiago de Compostela) for computational resources. J.M. thanks CONICYT for a Ph.D. fellowship; A.T.L. thanks the John Simon Guggenheim Memorial Foundation for a sabbatical fellowship. Repsol-YPF is also acknowledged for useful discussions about structure and experimental information.

## References and Notes

- (1) Small, B. L.; Brookhart, M.; Bennett, A. M. *J. Am. Chem. Soc.* **1998**, *120*, 4049.
- (2) Britovsek, G. J. P.; Gibson, V. C.; Wass, D. F. *Angew. Chem., Int. Ed. Engl.* **1999**, *38*, 428.

- (3) Britovsek, G. J. P.; Bruce, M.; Gibson, V. C.; Kimberly, B. S.; Maddox, P. J.; Mastroianni, S.; McTavish, S. J.; Redshaw, C.; Solan, G. A.; Strömberg, S.; White, A. J. P.; Williams, D. J. *J. Am. Chem. Soc.* **1999**, *121*, 8728.
- (4) Parr, R. G.; Yang, W. *Density-Functional Theory of Atoms and Molecules*; Oxford University Press: New York, 1989.
- (5) Geerlings, P.; De Proft, F.; Langenaeker, W. *Chem. Rev.* **2003**, *103*, 1793.
- (6) Morell, C.; Grand, A.; Toro-Labbé, A. *J. Phys. Chem. A* **2005**, *109*, 205.
- (7) Morell, C.; Grand, A.; Gutiérrez-Oliva, S.; Toro-Labbé, A. *Theoretical Aspects of Chemical Reactivity*; Toro-Labbé, A., Ed.; Elsevier: Amsterdam, 2007.
- (8) Britovsek, G. J. P.; Clentsmith, G. K. B.; Gibson, V. C.; Goodgame, D. M. L.; McTavish, S. J.; Pankhurst, Q. A. *Catal. Commun.* **2002**, *3*, 207.
- (9) Griffiths, E. A. H.; Britovsek, G. J. P.; Gibson, V. C.; Gould, I. R. *Chem. Commun.* **1999**, 1333–1334.
- (10) Khoroshun, D. V.; Musaev, D. G.; Vrenen, T.; Morokuma, K. *Organometallics* **2007**, *20*, 2001.
- (11) Bryliakov, K. P.; Semikolenova, N. V.; Zudin, V. N.; Zakhrov, V. A.; Talsi, E. P. *Catal. Commun.* **2004**, *5*, 45.
- (12) Kissin, Y. V.; Qian, C.; Xie, G.; Chen, Y. *J. Polym. Sci., Part A: Polym. Chem.* **2006**, *44*, 6159.
- (13) Knijnenburg, Q.; Gambarotta, S.; Budzelaar, P. H. M. *Dalton Trans.* **2006**, *46*, 5442.
- (14) Scott, J.; Gambarotta, S.; Korobkov, I.; Budzelaar, P. H. M. *J. Am. Chem. Soc.* **2005**, *127*, 13019.
- (15) Toro-Labbé, A. *J. Phys. Chem. A* **1999**, *103*, 4398.
- (16) Chattaraj, P. K. *J. Phys. Chem. A* **2001**, *105*, 511.
- (17) Pearson, R. G. *J. Chem. Ed.* **1987**, *64*, 561.
- (18) Mülliken, R. S. *J. Chem. Phys.* **1934**, *2*, 782.
- (19) Jaque, P.; Toro-Labbé, A. *J. Phys. Chem. A* **2000**, *104*, 995.
- (20) Chattaraj, P. K.; Gutiérrez-Oliva, S.; Jaque, P.; Toro-Labbé, A. *Mol. Phys.* **2003**, *101*, 2841.
- (21) Herrera, B.; Toro-Labbé, A. *J. Phys. Chem. A* **2004**, *108*, 1830.
- (22) Gutiérrez-Oliva, S.; Herrera, B.; Toro-Labbé, A.; Chermette, H. *J. Phys. Chem. A* **2005**, *109*, 1748.
- (23) Rincón, E.; Jaque, P.; Toro-Labbé, A. *J. Phys. Chem. A* **2006**, *110*, 9478.
- (24) Koopmans, T. A. *Physica* **1933**, *1*, 104.
- (25) Parr, R. G.; von Szentpaly, L.; Liu, S. *J. Am. Chem. Soc.* **1999**, *121*, 1922.
- (26) Parr, R. G.; Mortier, W. J. *J. Am. Chem. Soc.* **1986**, *108*, 5708.
- (27) Parr, R. G.; Yang, W. *J. Am. Chem. Soc.* **1984**, *106*, 4049.
- (28) Contreras, R.; Fuentealba, P.; Galván, M.; Pérez, P. *Chem. Phys. Lett.* **1999**, *304*, 405.
- (29) Yang, W.; Parr, R. G.; Pucci, R. *J. Chem. Phys.* **1984**, *81*, 2862.
- (30) Bulat, F. A.; Chamorro, E.; Fuentealba, P.; Toro-Labbé, A. *J. Phys. Chem. A* **2004**, *108*, 342.
- (31) Morell, C.; Grand, A.; Toro-Labbé, A. *Chem. Phys. Lett.* **2006**, *425*, 342.
- (32) Elango, M.; Subramanian, V.; Krishnamoorthy, B. S.; Gutiérrez-Oliva, S.; Toro-Labbé, A.; Roy, D. R.; Chattaraj, P. K.; Padmanabhan, J.; Parthasarathi, R. *J. Phys. Chem. A* **2007**, *111*, 9130.
- (33) Becke, A. D. *Phys. Rev. A* **1988**, *3*, 3098.
- (34) Perdew, J. P. *Phys. Rev. B* **1986**, *33*, 8822.
- (35) Delley, B. *J. Chem. Phys.* **1990**, *92*, 508.
- (36) Delley, B. *J. Chem. Phys.* **2000**, *113*, 7756.
- (37) *MaterialStudio*, version 4.0.; Accelrys Inc., 2005.
- (38) Becke, A. D. *J. Chem. Phys.* **1993**, *98*, 5648.
- (39) Lee, C.; Yang, W.; Parr, R. G. *Phys. Rev. B* **1988**, *37*, 785.
- (40) Miehlisch, B.; Savin, A.; Stoll, H.; Preuss, H. *Chem. Phys. Lett.* **1989**, *157*, 200.
- (41) Vosko, S. H.; Wilk, L.; Nusair, M. *Can. J. Phys.* **1980**, *58*, 1200.
- (42) Frisch, M. J.; Trucks, G. W.; Schlegel, H. B.; Scuseria, G. E.; Robb, M. A.; Cheeseman, J. R.; Montgomery, J. A., Jr.; Vreven, T.; Kudin, K. N.; Burant, J. C.; Millam, J. M.; Iyengar, S. S.; Tomasi, J.; Barone, V.; Mennucci, B.; Cossi, M.; Scalmani, G.; Rega, N.; Petersson, G. A.; Nakatsuji, H.; Hada, M.; Ehara, M.; Toyota, K.; Fukuda, R.; Hasegawa, J.; Ishida, M.; Nakajima, T.; Honda, Y.; Kitao, O.; Nakai, H.; Klene, M.; Li, X.; Knox, J. E.; Hratchian, H. P.; Cross, J. B.; Bakken, V.; Adamo, C.; Jaramillo, J.; Gomperts, R.; Stratmann, R. E.; Yazyev, O.; Austin, A. J.; Cammi, R.; Pomelli, C.; Ochterski, J. W.; Ayala, P. Y.; Morokuma, K.; Voth, G. A.; Salvador, P.; Dannenberg, J. J.; Zakrzewski, V. G.; Dapprich, S.; Daniels, A. D.; Strain, M. C.; Farkas, O.; Malick, D. K.; Rabuck, A. D.; Raghavachari, K.; Foresman, J. B.; Ortiz, J. V.; Cui, Q.; Baboul, A. G.; Clifford, S.; Cioslowski, J.; Stefanov, B. B.; Liu, G.; Liashenko, A.; Piskorz, P.; Komaromi, I.; Martin, R. L.; Fox, D. J.; Keith, T.; Al-Laham, M. A.; Peng, C. Y.; Nanayakkara, A.; Challacombe, M.; Gill, P. M. W.; Johnson, B.; Chen, W.; Wong, M. W.; Gonzalez, C.; Pople, J. A. *Gaussian 03*, Revision B.04.; Gaussian, Inc.: Wallingford, CT, 2003.
- (43) Herrera, B.; Toro-Labbé, A. *J. Phys. Chem. A* **2007**, *111*, 5921.
- (44) Toro-Labbé, A.; Gutiérrez-Oliva, S.; Murray, J. S.; Politzer, P. *Mol. Phys.* **2007**, *105*, 2619.
- (45) Pearson, R. G. *Chemical Hardness: Applications from Molecules to Solids*; Wiley-VCH, Verlag GMBH: Weinheim, 1997.
- (46) Pearson, R. G. *J. Chem. Educ.* **1987**, *64*, 561.
- (47) Pearson, R. G. *Acc. Chem. Res.* **1993**, *26*, 250.
- (48) Scott, J.; Gambarotta, S.; Korobkov, I.; Budzelaar, P. H. *Organometallics* **2005**, *24*, 6298.